ARTICLE

Ab initio study of metal carbide hydrides in 2.25Cr1Mo0.25V steel

Min He,[a] Chidozie Onwudinanti,[b] Yaoting Zheng,[c] Xiaomei Wu,[a] Zaoxiao Zhang*[a] and Shuxia Tao*[d]

Received 00th January 20xx,
Accepted 00th January 20xx

DOI: 10.1039/x0xx00000x

2.25Cr1Mo0.25V is the state-of the-art alloy used in the fabrication of modern hydrogenation reactors. Compared to the conventional 2.25Cr1Mo steel, 2.25Cr1Mo0.25V steel exhibits better performance, in particular higher hydrogen damage resistance. Previous experimental studies indicate that carbides in steels may be responsible for the hydrogen-induced damage. To gain a better understanding of the mechanism of such damage, it is essential to study hydrogen uptake in the metal carbides. In this study, Density Functional Theory (DFT) is used to investigate the stability of chromium, molybdenum and vanadium carbides (CrxCy, MoxCy and VxCy) in 2.25Cr1Mo0.25V steel. The stability of their corresponding interstitial hydrides was also explored. The results showed that the Cr_7C_3, Mo_2C and V_6C_5 are the most stable carbides in their respective metal-carbon (Cr-C, Mo-C and V-C) binary systems. Specifically, V_6C_5 shows the strongest hydrogen absorption ability because of the strong V-H and C-H ionic bonds. On the other hand, V_4C_3, whose presence in the alloy was established in experimental studies, is predicted to be stable as well, along with V_6C_5. Our finding indicate that the hydrogen absorption ability of V_4C_3 is higher than that of V_6C_5. Additionally, the charge and chemical bonding analyses reveal that the stability of the metal carbide hydride strongly depends on the electronegativity of the metal. Due to the high electronegativity of V, vanadium carbides form the strongest ionic bonds with hydrogen, compared to those of Mo and Cr. Rresults from this study suggest that the unique capacity of accommodating hydrogen in the vanadium carbides plays an important role in improved hydrogen damage resistance of 2.25Cr1Mo0.25V alloy in hydrogenation reactors.

1 Introduction

A hydrogenation reactor is a crucial component of a number of chemical and petrochemical production processes. It is widely used in hydrofining, catalytic hydrogenation and catalytic cracking units. The working conditions often entail high pressure, high temperature and a hydrogen-rich atmosphere. In such a harsh environment, hydrogen-induced cracking and failure of materials is a common problem. This not only affects the operating safety of hydrogenation reactor, but also has a great influence on the operating stability of other high-pressure equipment in the system. Various alloys have been designed for various specific operation conditions[1-3]. For example, austenitic stainless steels such as 304, 316, and 316L are generally used in the fabrication of hydrogen storage systems, and high strength steels such as Cr-Mo and 4130X steels are commonly used in high-pressure hydrogen vessels and pipelines. Hydrogen-induced cracking, caused by hydrogen-induced degradation of the mechanical properties, is one of the most common failure modes of these steels[4, 5]. Ductile-brittle fracture transition is a typical phenomenon for hydrogen embrittlement of steels in mechanical testing[6, 7]. Therefore, it is important to understand the reaction mechanism of hydrogen with the alloys.

2.25Cr1Mo is the most common alloy used in hydrogenation reactors in the last century[8]. However, with the aim of improving the production process, the working conditions of hydrogenation reactors have become harsher, and the material performance of 2.25Cr1Mo does not meet the requirements of new production processes[9]. Therefore, 2.25Cr1Mo0.25V has come to replace 2.25Cr1Mo, as it exhibits better high-temperature strength, creep resistance and hydrogen corrosion resistance. Experimental results showed that the hydrogen diffusivity in 2.25Cr1Mo0.25V is lower than in 2.25Cr1Mo steel, however, the hydrogen solubility is higher. It has been reported that the hydrogen-induced cracking modes of these two alloys are completely different[10-12]. Studies have found that hydrogen can be trapped by carbides and dislocations in the vanadium-modified alloy, resulting in coarser carbide grains in 2.25Cr1Mo0.25V steel[13, 14]. This indicates that the mechanisms of hydrogen influence in these two alloys are different, and carbides may play a significant role in improving hydrogen resistance of the vanadium-modified alloy. Although experiments indicate different mechanisms of hydrogen reaction with the two alloys, the interaction mechanism of hydrogen with the alloys at the atomic level is still unclear.

It is well established that chromium, molybdenum and vanadium are carbon-stable elements, and therefore tend to form carbides. Existing experimental results show that there are many forms of carbides in 2.25Cr1Mo0.25V steel. MC, M_2C, M_3C and M_7C_3, etc.[14-16] (where M = metal element) were found

[a] State Key Laboratory of Multiphase Flow in Power Engineering, School of Chemical Engineering and Technology, Xi'an Jiaotong University, No.28, Xianning West Road, Xi'an, Shaanxi, 710049, P.R. China. E-mail: zhangzx@xjtu.edu.cn
[b] Center for Computational Energy Research, DIFFER - Dutch Institute for Fundamental Energy Research De Zaale 20, 5612AJ Eindhoven, The Netherlands.
[c] School of science, Xi'an University of Architecture and Technology, No.13, Yanta Road, Xi'an Shaanxi, 710055, P.R. China.
[d] Center for Computational Energy Research, Department of Applied Physics, Eindhoven University of Technology, P.O. Box 513, 5600MB Eindhoven, The Netherlands. E-mail: s.x.tao@tue.nl

under different tempering treatments using transmission electron microscopy (TEM) and energy dispersive spectroscopy (EDS), with V and Nb in MC, Mo in M_2C, Fe in M_3C, and Cr and Fe in M_7C_3. Furthermore, experimental results showed hydrogen diffusivity and solubility tobe different in 2.25Cr1Mo and 2.25Cr1Mo0.25V. Lee[17] found, via slow rate tensile testing and thermal desorption spectrum analysis, that the role of vanadium carbides in hydrogen embrittlement resistance is different from that of chromium carbides and molybdenum carbides. The mechanism of vanadium carbide resistance to hydrogen embrittlement is by trapping hydrogen atoms, but that of chromium and molybdenum carbides is by inhibiting hydrogen atoms. Similarly, Chen *et al*[18] used atom probe tomography (APT) to investigate the distribution of hydrogen atoms in ferritic steel, and they were found to be trapped in vanadium carbides. The above analysis indicates that despite the fact they are the same class of compounds, the mechanism of hydrogen resistance of various carbides can be very different. Due to the difficulties in characterizing the atomic structure of such complex alloys experimentally, understanding the different interaction behaviours between hydrogen and various carbides remains challenging.

With the aim of explaining the stability of metal carbides and their influence on hydrogen embrittlement resistance, Density Functional Theory (DFT) was applied to investigate the stable structures of each M-C binary system, and compare hydrogen absorption ability of the preferred carbides. This study focuses on the behaviours of the possible carbides (CrxCy, MoxCy and VxCy) in 2.25Cr1Mo and 2.25Cr1Mo0.25Vsteel. We compare our calculations with existing experimental results, and discuss the structural stability of different carbon vacancies arranged in various types of carbides and their hydrogen uptake capacity. To understand the trends, one of the most stable structures, M_4C_3 (M=Cr, Mo, V), was used to compare the chemical bonding in the different carbides. Our results indicated that the stability of the metal carbide hydride strongly depends on the electronegativity of the metal. Due to the high electronegativity of V, vanadium carbides form the strongest ionic bonds with hydrogen, compared to those of Mo and Cr.

2 Methods

The calculations were carried out using DFT and implemented in the Vienna Ab-initio Simulation Package (VASP)[19]. Exchange correlation was corrected by the generalized gradient approximation (GGA) of Perdew-Burke-Ernzerhof (PBE)[20]. For the M-C binary system, convergence tested on the key parameters of each structure are preformed, such as lattice parameters, kinetic energy cutoff, and k-mesh, which are all listed in Table S1. The calculated lattice constants of Cr, Mo and V are 2.85 Å, 3.16 Å and 3.00 Å, respectively. These calculated results agree well with the corresponding experimental results, 2.88 Å, 3.15 Å and 3.02 Å[21-23]. Magnetic state of Cr and V may play a role in determine the thermodynamics properties of these metals. Therefore, Spin-polarized DFT calculations were done and the results show magnetic moment of 0 and almost unchanged total energies for both metals. However, it should be noted that the current DFT description may give rise to small uncertainties in the calculated energetics due to the fact the standard DFT cannot take into account of the magnetic entropy contribution[24]. The magnetic moment of Cr is 0. Vanadium, as well as the diamond and graphite carbon structures have no magnetic ordering[25], so magnetism was not considered in the computations. Gamma-centered k-point grids were used in all calculations. The tetrahedron method with Blöchl corrections was used for energy calculations, and the first-order Methfessel-Paxton smearing is used for structure optimization. The convergence criteria for energies in electronic self-consistent-loop and forces in the ionic relaxation loop were set to $1E^{-5}$ eV/atom and 0.01 eV/Å, respectively.

The formation enthalpy of the M-C binary system and the formation enthalpy of hydrogen in carbides are calculated per Equations (1) and (2).

$$\Delta E_f = \frac{E_{M_xC_y} - \left(xE_M + yE_C\right)}{x+y} \quad (1)$$

$$\Delta E_H = \frac{E_{M_xC_yH_n} - \left(E_{M_xC_y} + \frac{n}{2}E_{H_2}\right)}{\frac{n}{2}} \quad (2)$$

where $E_{M_xC_y}$, E_M and E_C are the total energy of metal carbide, the energy per metal atom in equilibrium state and the energy per carbon atom, respectively. The terms x and y represent the number of metal atoms and the number of carbon atoms, respectively. Additionally, $E_{M_xC_yH_n}$ is the total energy of hydrogen atom absorbed in metal carbides, E_{H_2} is the total energy of hydrogen molecule, and n is the number of hydrogen atoms.

To explain the trends found in the hydrogen absorption energy in various metal carbides, Bader atomic volumes and charges[26-29] were used, as well as Density Derived Electrostatic and Chemical (DDEC6) net atomic charge and bond orders[30, 31]. The Bader charge is a measure of the charge transfer, while the Bader volume is an indication of how closely the charge associated with each atom is localized around the nucleus. The covalent nature is indicated by the DDEC6 bond order, with a higher value showing a stronger covalent bond. The sum of bond orders for each atom, i.e. its total bond order, is an indication of the activity of the atom in that particular configuration. The ionic contribution of a bond can be characterized by net atomic charge, which quantifies the charge transfer between atoms[32]. Lastly, charge density differences were used to analyze the charge transfer in carbide formation, as described by Equation (3),

$$\Delta\rho = \rho_{AB} - \rho_A - \rho_B \quad (3)$$

where ρ_{AB} is the charge density of the system, and ρ_A, ρ_B are the charge densities of the components in isolation, respectively.

3 Results and discussion

3.1 The stability of carbides in metal-carbon binary systems

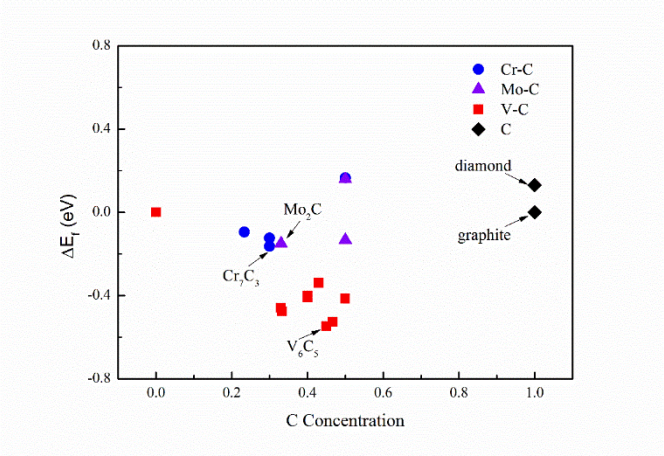

Figure 1 Formation enthalpies of MxCy (M = Cr, Mo, V) binary system. The most stable compositions for each systems are marked with arrows.

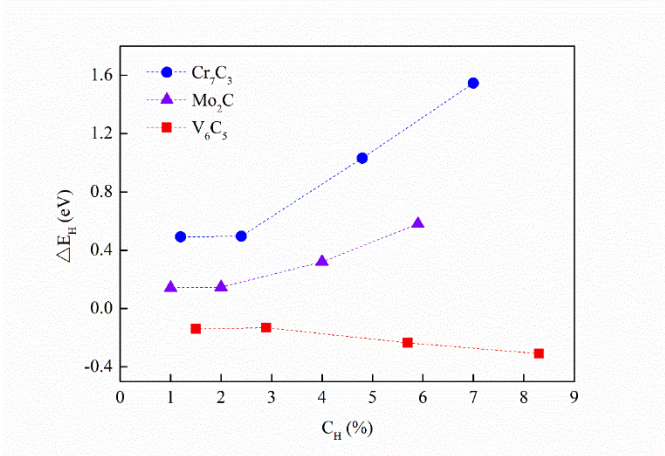

Figure 3 The formation enthalpies of interstitial hydrogen in metal carbides with different hydrogen concentrations.

Previous experimental measurement using TEM[16] shows that the most abundant carbides in 2.25Cr1Mo0.25V are MC, M_2C, M_7C_3 and $M_{23}C_6$. The formation enthalpies are calculated for the most typical metal carbides including those of chromium in the forms of $Cr_{23}C_6$(Fm-3m), Cr_7C_3(Pnma), Cr_7C_3(P63mc), CrC(Fm-3m), molybdenum in the forms of Mo_2C(Pbcn), MoC(P6m2), MoC(Fm-3m) and vanadium in the forms of V_2C(P63/mmc), V_2C(Pbcn), V_3C_2(R-3m), V_4C_3(Fm-3m), V_6C_5(P3112), V_8C_7(P4132) and VC(Fm-3m). The calculated energies are shown in Figure 1. Two carbon structures are used to calculate the formation enthalpy in Figure 1, for two stable forms of carbon: graphite (P63/mmc) and diamond (Fd-3m). We chose diamond as a reference for carbon[33].

As shown in Figure 1, the majority of the carbides are energetically favourable (with negative formation energies) including $Cr_{23}C_6$(Fm-3m), Cr_7C_3(P63mc), Cr_7C_3(Pnma), Mo_2C(Pbcn), MoC(P6m2) and all vanadium carbides. Comparing all compositions for each type of metal carbides, Cr_7C_3(Pnma), Mo_2C(Pbcn) and V_6C_5(P3112) are the most stable structures for their respective metals. The lattice structure for each system is shown in Figure 2.

In addition to metal carbides, carbon atom may also exist in solute state in metal lattice. Cr, Mo and V all have crystal structure of body centred cubic (bcc) and two kinds of interstitial site can be found, i.e. octahedral site(o-site) and tetrahedral site(t-site). The calculated formation enthalpies of one carbon atom in the interstitial site show t-site is more stable than o-site. The value of formation enthalpies of one carbon atom in Cr, Mo, V unit cells are 1.72 eV, 1.60 eV and 0.91 eV, respectively. The very large positive formation energies can be understood by analyzing the lattice structures of iron matrix. The lattice constant of bcc-Fe is 2.84 Å, the radiuses of two interstitial sites, o-site and t-site, are 0.190 Å and 0.358 Å, respectively. Compared with atomic radius of Cr, Mo, V and C (shown in Table 4), the interstitial site of bcc-Fe is too small to accommodate carbon atoms. This means that carbon atom cannot be stabilized in metal lattice. Compared with the negative formation enthalpy of metal carbides shown in Figure 1, it is clear that the formation of metal carbides is much more favorable than the formation of solute state of carbon atom in metal.

3.2 Hydrogen absorption in metal carbides

After establishing the most stable compositions of the metal carbides (Cr_7C_3, Mo_2C and V_6C_5 as shown in Figure 2), the hydrogen absorption in these structures was investigated. In order to compare hydrogen absorption ability in the lowest-energy carbide, simple unit cells of Cr_7C_3, V_6C_5, and a 2×2×1 supercell Mo_2C structures were used. These cells are chosen to

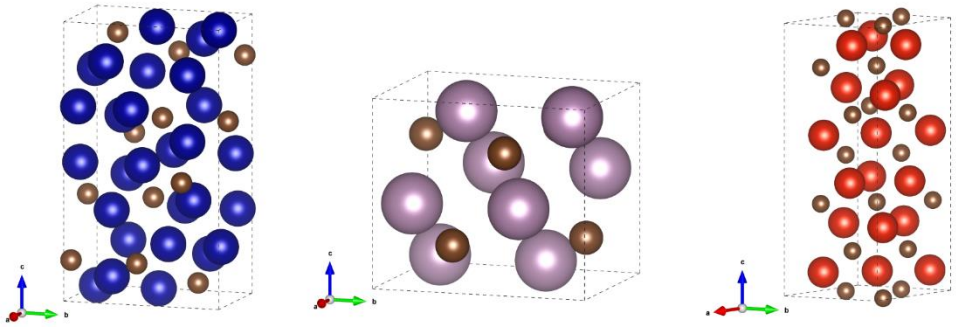

(a) Cr_7C_3(Pnma) (b) Mo_2C(Pbcn) (c) V_6C_5(P3112)

Figure 2 Simple unit cell of three most stable metal carbides. Blue, purple, red and brown spheres represent Cr, Mo, V and C atoms, respectively. Pnma, Pbcn and P3112 in the brackets are their space group.

have the hydrogen concentrations in the carbides at similar levels while keeping the computational load manageable.

In Cr_7C_3, there are two kinds of t-site. One is hydrogen atom in 4c site, and another one is 8d site. The energy of 8d site is 0.25 eV, which is higher than that of the former one. In Mo_2C, the o-site and t-site are possible for a hydrogen atom, with the energy at the t-site 0.48 eV lower than that of the o-site. In V_6C_5, there is just one kind of t-site. Table 1 lists the lowest formation enthalpies of hydrogen in interstitial site of each carbide. It can be observed that although the hydrogen concentration in V_6C_5 is the highest in all the calculated structures, the formation enthalpy of hydrogen is the lowest, and V_6C_5 has the only negative value. These formation enthalpies are affected by the presence of compressive or tensile strain, which may be imposed on the carbide structures by the surrounding Fe matrix. The changes are discussed briefly in the supplementary material.

This result shows that vanadium carbide has better hydrogen absorption ability than chromium carbide and molybdenum carbide. Considering the effect of hydrogen concentration on hydrogen formation enthalpy, Figure 3 shows that the interstitial hydride formation enthalpies of Cr_7C_3 and Mo_2C increase with hydrogen concentration, while that of V_6C_5 falls slightly. When the hydrogen concentration is lower than 3%, the formation enthalpies have no changes. Based on these results, we conclude that hydrogen concentration affects the hydride formation enthalpy, but it does not change the hydrogen absorption performance of the different carbides relative to one another. Vanadium carbide remains the best hydrogen absorber at all the calculated concentrations.

To understand the underlying reason for the differences in absorption energy of hydrogen in the three carbides, the volume, net atomic charge (NAC) and bond order of the hydrogen atom in Cr_7C_3, Mo_2C and V_6C_5 were calculated. The results are listed in Table 1. The void volume in the t-site of V_6C_5 is 1.7 times larger than that of the o-site in Mo_2C, and 1.9 times larger than that of t-site in Cr_7C_3, indicating that more space is available for a hydrogen atom in V_6C_5. From the net atomic charge (NAC), it is apparent that the metal atoms gain charge while carbon and hydrogen atoms lose charge. It can be observed that V in $(V_6C_5)_3H$ gains more charge than Cr in $(Cr_7C_3)_4H$ and Mo in $(Mo_2C)_{16}H$, while C and H atoms in $(V_6C_5)_3H$ lose more charge compared with that in $(Cr_7C_3)_4H$ and $(Mo_2C)_{16}H$. Specifically, the H atom in vanadium carbides loses double the amount of charge compared to the other two carbides. The bond order analysis shows a slight decrease in the covalent bonding of the V-H compared with that of Mo and Cr, while all the bond orders of C-H are very small. The latter is ascribed to the fact that the interstitial sites are surrounded by metal atoms, so the C-H interaction is relatively small. Indeed, the distance between a C atom and an H atom in chromium carbide, molybdenum carbide and vanadium carbide is about 2.5 Å, 2.5 Å, and 3 Å, respectively. The distance is too big to form strong covalent bonds. The ionic bond therefore plays a more important role than that of the covalent in the hydrogen absorption of metal carbides. The strong ionic bonding of V-C and C-H in $(V_6C_5)_3H$ explains the absorption of hydrogen in V_6C_5 being the most favourable among the metal carbides investigated here.

3.3 Other vanadium carbides

As discussed above, V_6C_5 is the most stable vanadium carbide and it has the strongest hydrogen absorption ability among all three metal carbides. However, previous experimental studies have clearly identified VC as the most abundant species in 2.25Cr1Mo0.25V steel[15, 16]. Takahashi[35] analyzed the atomic ratio of V and C in vanadium carbide and pointed out that the chemical composition of vanadium carbide is V_4C_3, which has the same structure as NaCl, but with a carbon vacancy. In our DFT calculations, the V_4C_3 lattice structure is formed by removing a C atom from a VC unit cell. Most previous studies[36, 37] focused on the mechanical properties of the vanadium carbides, and did not extensively discuss the stability of the alloys. Chong *et al*.[38] summarized the formation enthalpies of V-C binary compounds, and found that the most stable phase is V_6C_5. These results are consistent with our calculations. As shown in Figure 1, although VC is a stable structure, its formation energy is -0.48 eV, which is higher than that of V_6C_5. Therefore, further analysis of the stability of vanadium carbides is needed.

The structure of VC is NaCl type with lattice constant a = 4.16 Å. Each unit contains 4 vanadium atoms and 4 carbon atoms. Vanadium atoms fill in 4a sites and carbon atoms fill in 4c sites. By removing one carbon from a VC unit cell, V_4C_3 can be obtained, maintaining a cubic rock-salt type structure but with a slightly smaller lattice constant of a = 4.12 Å. Figure 4 shows 2×2×2 supercell structures of V_4C_3 in three possible configurations including one regular (Figure 4(b)) and two irregular (Figure 4(c) and Figure 4(d)) structures. The irregular structures have the vacancies distributed in a disordered, asymmetrical manner throughout the cell. The regular V_4C_3 structure in Figure 4(b) was obtained by removing one carbon atom in a VC unit cell. For comparison, the formation energy of V_4C_3 is 0.08 eV and 0.21 eV higher than that of VC and V_6C_5, respectively. In fact, it is the highest among all vanadium

Table 1 The formation enthalpies of hydrogen in Cr7C3(Pnma), Mo2C(Pbcn) and V6C5(P3112).

	C_H [%]	H atom position	ΔE_H [eV]	H atom volume [Å^3]	Net atomic charge			Bond order	
					M	C	H	M-H	C-H
$(Cr_7C_3)_4H$	2.4	t-site	0.50	3.21	0.51	-1.01	-0.23	0.31	0.02
$(Mo_2C)_{16}H$	2.0	o-site	0.15	3.67	0.48	-0.86	-0.20	0.22	0.02
$(V_6C_5)_3H$	2.9	t-site	-0.13	6.09	1.31	-1.44	-0.48	0.17	0.03

Note: C_H is the hydrogen concentration in each bulk cell. Net atomic charge is the average charge of metal or carbon atoms close to the hydrogen atoms. Bond order is calculated between the metal or carbon atoms and hydrogen atoms.

Table 2 The formation enthalpies of different vacancies arrangement of V_4C_3 structures.

Weighting	Amount	ΔE_f[eV]		Weighting	Amount	ΔE_f[eV]		Weighting	Amount	ΔE_f[eV]	
4	1	-0.39	-	96	23	-0.58	-0.58	512	2	-0.55	-0.53
12	2	-0.49	-0.44	128	4	-0.56	-0.56	768	1559	-0.56	-0.56
24	2	-0.53	-0.50	192	99	-0.57	-0.57	1536	5958	-0.57	-0.56
32	2	-0.56	-0.57	256	4	-0.54	-0.49				
48	9	-0.57	-0.46	384	378	-0.57	-0.55				

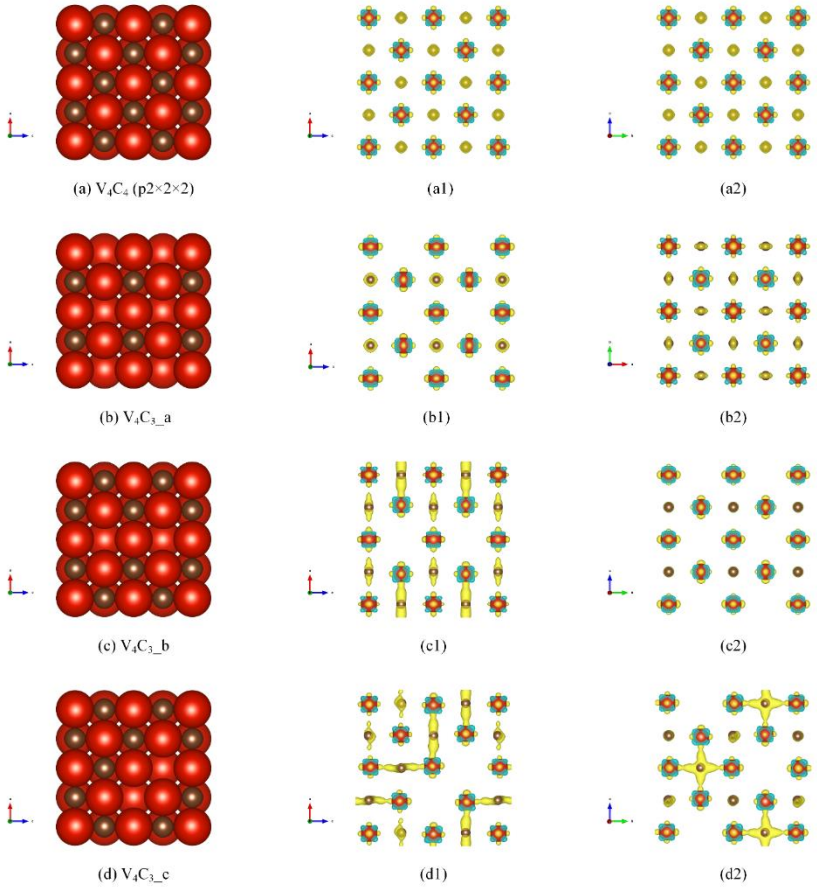

Figure 4 (a) is NaCl structures of VC, (b)-(d) are three possible V_4C_3 structures with different distribution of carbon vacancies. (b) is for ordered carbon vacancies, (c) and (d) are for disordered carbon vacancies. Red and brown spheres are vanadium and carbon atoms respectively. (a1-d1) and (a2-d2) are images of second order difference in charge density from side views, respectively. The isosurface of electron density in the yellow region is -0.02 e/Å^3, which stands for the electron accumulation. The isosurface of charge density in the cyan region is 0.02 e/Å^3, which stands for charge depletion.

carbides (as discussed at Section 3.1).

For irregular structures, there are 32 vanadium atoms and 24 carbon atoms in each structure. V_4C_3 is created by removing one carbon atom from VC (V_4C_4) structure. Thus in 2×2×2 supercell VC structure, 8 carbon atoms should be removed to create V_4C_3 lattice. This means that there are C_{32}^{8} possible V_4C_3 structures. In addition, 8043 possible structures can be obtained with the stoichiometry of V_4C_3. All structures can be classified in 13 categories by the weighting value. The weighting value represents the number of same structures, and the amount represents the number of the same weighting. Two out of each category were chosen, and the formation energies were calculated, which are listed in Table 2. The structures with uniformly distributed carbon vacancies have the highest energy (-0.39 eV, Figure 4(b)). However, the formation energy of the other nine structures of V_4C_3 is close to that of V_6C_5 (0.03 or 0.04 eV higher than that of V_6C_5 (-0.61 eV)), which implies that most V_4C_3 structures are nearly as stable as V_6C_5. The irregular V_4C_3 structures (see Figure 4(c) and (d) for two example) show irregular arrangements of carbon vacancies, where carbon vacancies were created randomly in the lattice of VC. This could explain why V_4C_3 is not easily detected from VC using experimental characterizations, such as TEM and EDS[14, 15].

The formation enthalpy of V_4C_3 decreases from Figure 4 (b) to (d), at -0.39 eV, -0.49 eV, -0.58 eV, respectively. The electron density difference analysis was performed to understand such trends found in energies. In all structures, we generally observe electron density accumulation around the carbon atom, and we see that vanadium atoms accumulate electron density in the region between them and carbon atoms in the same plane but deplete charge in the region between them and carbon atoms in neighbouring planes. Figure 4(a) shows that the electron density difference in VC distributed regularly. In Figure 4(b), the charge around carbon atoms accumulates only in the direction from carbon atoms to vacancies. There is more electron density accumulating between carbon and vanadium atoms in Figure 4(c) and (d) because of greater irregularity in the distribution of vacancies from Figure 4(b) to (d). However, the loss of electron density around vanadium atom is similar in these structures, which indicates that the vacancies could change the electron density distribution around carbon atoms. The NAC of VC is 1.48 for vanadium atom and -1.48 for carbon atom. However, in V_4C_3, i.e. Figure 4(d), there are two kinds of vanadium atoms: one whose neighbour has just one vacancy, with NAC 1.15; and another whose neighbour has two vacancies (the vanadium atom in the middle site), with NAC 0.91. For the carbon atom, there are three kinds of charge distribution: with two small lobes (the second atom in the first row of Figure 4(d1)), NAC is -1.47; with two large lobes (the third atom in the second row of Figure 4(d1)), NAC is -1.36; and with four lobes, net atomic charge is -1.29. These results suggest that the ionic effect becomes weaker, while the covalent bond should be stronger, and these have been verified by bond order results. To conclude, covalent bonds between carbon and vanadium atoms can be enhanced when the irregularity of vacancy arrangement increases. This is why most V_4C_3 structures are more stable than that of VC structures.

3.5 The formation of metal carbide hydrides

In order to understand the influence of the distribution of vacancies, the formation enthalpies of hydrogen in the above one regular and two irregular V_4C_3 structures (Figure 4(b)-(d)) were calculated. For better comparison of the effect of the type of metal atoms in metal carbides on their hydrogen absorption ability, the formation enthalpies of hydrogen in Cr_4C_3 and Mo_4C_3 were also calculated. All results are summarized in Figure 5. According to Bravo *et al.*[39], considering entropy at 300 K, the vibration entropy of V_4C_3 is 0.0145 eV and configurational entropy of hydrogen atom in V_4C_3 is 0.0096 eV, respectively. These values are much smaller than the formation enthalpies of hydrogen. Therefore, entropy is not explicitly considered here.

The formation enthalpies of M_4C_3 decrease from the M_4C_3_a to the M_4C_3_c structure, with the vacancy arrangement becoming more disordered, and the formation enthalpies of hydrogen increasing. The bond order of carbon-hydrogen and total NAC of hydrogen are similar in three structures, which are 0.02 and -0.51, respectively. The bond order of hydrogen-vanadium is 0.23 in M_4C_3_a structure. However, in M_4C_3_b and M_4C_3_c, the bond order of vanadium-hydrogen becomes more complicated due to the irregular arranged of vacancies and the

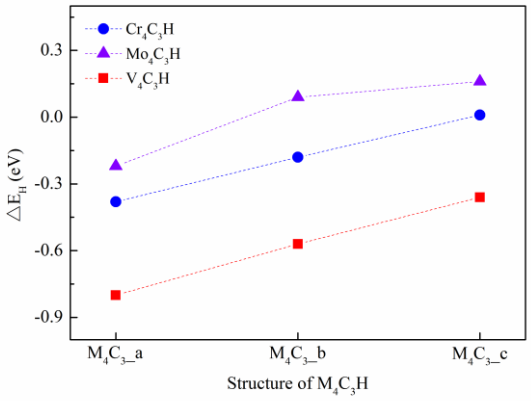

Figure 5 The formation enthalpies of hydrogen in M4C3H system. The labels in the horizontal axis match with that in Figure 4.

difference in the number of vanadium atoms around hydrogen atoms. The irregular distributed vacancies also affect the charge distribution around vanadium and carbon atoms. Similar results are also shown in hydrogen-chromium and hydrogen-molybdenum in Cr_4C_3 and Mo_4C_3 structures. This means that the metal atom plays a significant role in hydrogen absorption performance.

In the V_4C_3 unit cell, the concentration of hydrogen is 12.5% and the hydrogen formation enthalpy is -0.80 eV, while one hydrogen atom occupies carbon vacancy, as shown in Figure 5. At the meantime, in V_6C_5 simple cell, even though all interstitial sites are occupied by hydrogen atoms, the concentration of hydrogen is 8.3%, and hydrogen formation enthalpy is -0.31 eV, as shown in Figure 3. This value is higher than in V_6C_5, as shown in Table 1 (2.9%). Based on the above results, with the hydrogen concentration in V_4C_3 higher than in V_6C_5, but the formation enthalpy of hydrogen lower than in V_6C_5, we conclude that V_4C_3 has better hydrogen absorption ability than V_6C_5.

To give a clear explanation of hydrogen absorption ability of carbides, the formation enthalpies of Cr_4C_3H, Mo_4C_3H and V_4C_3H with the same lattice structure are calculated. The lattice constants of Cr_4C_3H, Mo_4C_3H and V_4C_3H are 4.064 Å, 4.365 Å and 4.1608 Å, respectively. The results of NAC and bond order calculations are displayed in Table 3. As shown in Table 3, the void radii are similar in Cr_4C_3 and V_4C_3 structures; however, they are smaller than in the Mo_4C_3 structure. This is because chromium and vanadium are elements in the fourth period, whereas the molybdenum is in the next period and the same group as chromium. When hydrogen atoms are absorbed in the metal carbide, metal atoms lose electrons, while carbon and hydrogen atoms gain electrons. Furthermore, the NACs in the three metal carbides are different. However, the bond orders of metal-hydrogen interaction are very close, which indicates that the ionic bond plays a predominant role in the hydrogen absorption ability for metal carbides. In comparison with molybdenum and chromium carbides in the steels, the

Table 3 The void radius, net atomic charge and bond order of H atom in M_4C_3H system.

	H atom void radius [Å]	Net atomic charge			Bond order	
		M	C	H	M-H	C-H
Cr_4C_3H	0.74	0.91	-1.25	-0.42	0.22	0.02
Mo_4C_3H	0.78	0.72	-1.07	-0.33	0.24	0.01
V_4C_3H	0.73	1.05	-1.41	-0.52	0.23	0.02

Note: Net atomic charge is the average charge of metal or carbon atoms close to the hydrogen atoms. Bond order is calculated between the metal or carbon atoms and hydrogen atoms.

Table 4 The atomic radius[35] and Pauling electronegativity[40] of H, V, Cr, Mo and C elements.

Period	Group			
	IA	VB	VIB	IVA
1	$H_{2.20}^{37}$			
2				$C_{2.55}^{77}$
4		$V_{1.63}^{135}$	$Cr_{1.66}^{129}$	
5			$Mo_{2.16}^{140}$	

Note: The superscript is atomic radius, the unit is pm; the subscript is Pauling electronegativity.

vanadium carbides form the most stable hydrides under hydrogen environment.

The above analysis also agrees well with the elements' Pauling electronegativity. Due to the fact that carbon and hydrogen atoms have higher electronegativity than Cr, Mo and V atoms, electron pairs will shift towards the C and H atom in carbide. Therefore, the NAC of C and H atoms shows negative and the net atomic charge of metal atoms exhibits positive. When comparing the electronegativity among Cr, Mo and V atoms, the vanadium shows the lowest value. Therefore, the strength of ionic bonds between V atoms and H, C atoms is strong, much higher than that between C atoms and Cr, Mo atoms.

4 Conclusions

In this study, the hydrogen absorption ability of metal carbides in 2.25Cr1Mo and 2.25Cr1Mo0.25V steel were investigated via DFT calculations. Among all possible compositions, Cr_7C_3, Mo_2C and V_6C_5 were predicted to be the most stable carbides for each of the metal species. A comparison of the formation enthalpies of the three metal carbide hydrides shows that V_6C_5 has the strongest hydrogen absorption ability. Another stable vanadium carbide, V_4C_3, was also investigated and compared with that of V_6C_5. The DFT results show that the stability of V_4C_3 is very close to that of V_6C_5. In a word, vanadium carbides show better hydrogen absorption performance than that of chromium carbides and molybdenum carbides. Further charge and bonding analyses reveal that the hydrogen absorption ability of metal carbides is determined by the strength of the ionic bonds in the systems. Such ionic bonds are strongly correlated with the electronegativity of the metals. Among all the metals (Cr, Mo and V), the lowest electronegativity of the V atom undoubtedly results in the strongest ionic bonds forming in vanadium carbide hydrides, leading to stronger hydrogen absorption ability than that of chromium and molybdenum carbides. The highly-favourable formation of vanadium carbide hydrides has important implications for the improvement of hydrogen resistance of 2.25Cr1Mo0.25V steel. Having established such thermodynamic factors, future work will be performed to investigate the kinetics of hydrogen diffusion in the different metal carbides, as well as the effects of defects and imperfections on the behaviour of hydrogen in the steel.

While the current study focuses on the thermodynamics of hydrogen in metal carbides, future work focusing on the kinetics of hydrogen diffusion would shed light on the overall impact of hydrogen in these systems. Further study of the behavior of hydrogen in iron matrix and its comparison within those metal carbides can lead to a comprehensive understanding of the mechanisms of hydrogen induced damage in steel.

Conflicts of interest

There are no conflicts to declare.

Acknowledgements

The authors would like to acknowledge the support from the National Natural Science Foundation of China (No.11902241), the National Basic Research Program of China (No. 2015CB057602), Youth Science Foundation of Shaanxi Province (2020JQ-058), and the computation support from Eindhoven University of Technology. Moreover, the authors are very much thankful to Mr. Zulqarnain Mushtaq for formatting and proofreading. S. Tao acknowledges funding supported by the Computational Sciences for Energy Research (CSER) tenure track program of Shell and NWO, the Netherlands (project number 15CST04-2).

Notes and references

1 Y. Zheng, C. Zhou, Y. Hong, J. Zheng and L. Zhang, *Materials Research Express*, 2018, **5**, 056524.
2 X. Chen, L. Ma, C. Zhou, Y. Hong, H. Tao, J. Zheng and L. Zhang, *Corrosion Science*, 2019, **148**, 159-170.
3 T. C. Cui, P. F. Liu, J. Y. Zheng and C. H. Gu, *Journal of Failure Analysis and Prevention*, 2016, **16**, 770-782.
4 Y. Fukai, *The Metal-Hydrogen System Basic Bulk Properties*, Springer Berlin Heidelberg, Berlin, Heidelberg, 2005.
5 S. Zhu, C. Zhang, Z. Yang and C. Wang, *Nuclear Engineering and Technology*, 2017, **49**, 1748-1751.
6 N. Zan, H. Ding, X. Guo, Z. Tang and W. Bleck, *International Journal of Hydrogen Energy*, 2015, **40**, 10687-10696.
7 J. A. Donovan, presented in part at the Conference on understanding environmental degradation of engineering materials, Blacksburg, Virginia, USA, 1975-06-23, 1975.
8 A. P. Institute, in *API RP 941*, American Petroleum Institute, Washington2016.
9 Z. Liu, J. Chen, H. Bu and X. Chen, *China Pressure Vessel Technology*, 2011, **28**, 33-40.
10 A. M. Brass, F. Guillon and S. Vivet, *Metallurgical and Materials Transactions A*, 2004, **35**, 1449-1464.
11 R. C. Brouwer, *International Journal of Pressure Vessels and Piping*, 1993, **56**, 133-148.

12 L. F. Lemus, J. H. Rodrigues, D. S. Santos and L. H. Almeida, *Defect and Diffusion Forum*, 2009, **283-286**, 370-375.
13 Y. Wang, G. Cheng, M. Qin, Q. Li, Z. Zhang, K. Chen, Y. Li, H. Hu, W. Wu and J. Zhang, *International Journal of Hydrogen Energy*, 2017, **42**, 24549-24559.
14 Z. Yongtao, H. Haibo, M. Lede, Z. Hanqian and L. Jinfu, *Materials Characterization*, 2009, **60**, 953-956.
15 Z. Jiang, P. Wang, D. Li and Y. Li, *Materials Science and Engineering: A*, 2017, **699**, 165-175.
16 A. L. Cardenas, R. O. Silva, C. B. Eckstein and D. S. dos Santos, *International Journal of Hydrogen Energy*, 2018, **43**, 16400-16410.
17 J. Lee, T. Lee, D. Mun, C. M. Bae and C. S. Lee, *Scientific Reports*, 2019, **9**, 5219.
18 Y. S. Chen, D. Haley, S. S. A. Gerstl, A. J. London, F. Sweeney, R. A. Wepf, W. M. Rainforth, P. A. J. Bagot and M. P. Moody, *Science*, 2017, **355**, 1196-1199.
19 G. Kresse and J. Furthmüller, *Physical Review B*, 1996, **54**, 11169-11186.
20 G. Kresse and D. Joubert, *Physical Review B*, 1999, **59**, 1758-1775.
21 H. W. King, *Bulletin of Alloy Phase Diagrams*, 1983, **4**, 449-450.
22 G. Brauer and W. D. Schnell, *Journal of the Less Common Metals*, 1964, **6**, 326-332.
23 G. Chiarotti, in *Interaction of Radiation with Surfaces and Electron Tunneling*, ed. G. Chiarotti, Springer-Verlag Berlin Heidelberg1996, vol. 24D.
24 F. Körmann, B. Grabowski, P. Söderlind, M. Palumbo, S. G. Fries, T. Hickel and J. Neugebauer, *Journal of Physics: Condensed Matter*, 2013, **25**, 425401.
25 A. Jain, S. P. Ong, G. Hautier, W. Chen, W. D. Richards, S. Dacek, S. Cholia, D. Gunter, D. Skinner, G. Ceder and K. A. Persson, *APL Materials*, 2013, **1**, 011002.
26 W. Tang, E. Sanville and G. Henkelman, *Journal of Physics: Condensed Matter*, 2009, **21**, 084204.
27 E. Sanville, S. D. Kenny, R. Smith and G. Henkelman, *Journal of computational chemistry*, 2007, **28**, 899-908.
28 G. Henkelman, A. Arnaldsson and H. Jónsson, *Computational Materials Science*, 2006, **36**, 354-360.
29 M. Yu and D. R. Trinkle, *The Journal of Chemical Physics*, 2011, **134**, 064111.
30 T. A. Manz and N. G. Limas, *RSC Advances*, 2016, **6**, 47771-47801.
31 T. A. Manz, *RSC Advances*, 2017, **7**, 45552-45581.
32 C. Onwudinanti, I. Tranca, T. Morgan and S. Tao, *Nanomaterials (Basel)*, 2019, **9**, 129.
33 A. Dick, F. Körmann, T. Hickel and J. Neugebauer, *Physical Review B*, 2011, **84**, 125101.
34 M. Sluiter, *MRS Proceedings*, 2006, **979**, 0979-HH0914-0903.
35 J. Takahashi, K. Kawakami and T. Tarui, *Scripta Materialia*, 2012, **67**, 213-216.
36 H. Liu, J. Zhu, Y. Liu and Z. Lai, *Materials Letters*, 2008, **62**, 3084-3086.
37 B. Wang, Y. Liu and J. Ye, *Physica Scripta*, 2013, **88**, 015301.
38 X. Chong, Y. Jiang, R. Zhou and J. Feng, *RSC Advances*, 2014, **4**, 44959-44971.
39 F. Brivio, C. Caetano and A. Walsh, *The Journal of Physical Chemistry Letters*, 2016, **7**, 1083-1087.
40 J. E. Huheey, E. A. Keiter and R. L. Keiter, *Inorganic chemistry: principles of structure and reactivity, 4th ed.*, Harper Collins College Publishers, New York, 1993.

Table S 1 Basic calculation parameters and per atom energy of metal-carbon systems.

	Space group	Lattice parameters [Å]	E_{cut} [eV]	K-mesh	E_M [eV]	ΔE_f [eV]
C(diamond)	Fd-3m	2.53×2.53×2.53	500	8×8×8	-9.09	
C(graphite)	P63/mmc	2.47×2.47×7.91	500	8×8×2	-9.22	
Cr	Im-3m	2.85×2.85×2.85	500	8×8×8	-9.51	
Mo	Im-3m	3.16×3.16×3.16	400	10×10×10	-10.92	
V	Im-3m	3.00×3.00×3.00	500	10×10×10	-8.96	
$Cr_{23}C_6$	Fm-3m	10.54×10.54×10.54	700	2×2×2		-0.09
Cr_7C_3	Pnma	4.50×6.88×12.09	700	5×3×2		-0.16
Cr_7C_3	P63mc	13.87×13.87×4.49	700	2×2×10		-0.12
CrC	Fm-3m	4.06×4.06×4.06	450	8×8×8		0.17
Mo_2C	Pbcn	4.74×6.06×5.22	800	12×12×12		-0.15
MoC	P6m2	2.92×2.92×2.82	800	9×9×9		-0.13
MoC	Fm-3m	4.37×4.37×4.37	500	8×8×8		0.16
V_2C	P63/mmc	2.89×2.89×4.53	450	10×10×5		-0.46
V_2C	Pbcn	4.55×5.73×5.04	450	8×8×8		-0.48
V_3C_2	R-3m	2.92×2.92×27.80	450	8×8×1		-0.41
V_4C_3	Fm-3m	4.12×4.12×4.12	500	8×8×8		-0.34
V_6C_5	P3112	5.10×5.10×14.36	500	10×10×2		-0.55
V_8C_7	P4132	8.34×8.34×8.34	500	6×6×6		-0.53
VC	Fm-3m	4.16×4.16×4.16	500	8×8×8		-0.41

Table S 2 The formation enthalpies and hydrogen formation enthalpies of metal carbides in the original, compressed and tense lattices.

Stress	$\triangle E_f$ [eV]			$\triangle E_H$ [eV]		
	Cr_7C_3	Mo_2C	V_6C_5	$(Cr_7C_3)_4H$	$(Mo_2C)_{16}$ H	$(V_6C_5)_3H$
Origin	-0.163	-0.150	-0.548	0.496	0.146	-0.131
Compressed	0.161	0.160	-0.350	1.314	0.602	-0.041
Tense	0.061	0.060	-0.412	-0.091	-0.131	-0.081

Above we report the results of calculations to study the effect of strain on metal carbide hydrogen absorption, in Table S2. The original structure is the relaxed lattice structure, the compressed structure has a lattice constant 95% of the original, and the tensile structure is extended to 105%. It can be observed that the strain raises the formation enthalpy for the carbides; both compression and tension change the formation enthalpy of Cr_7C_3 and Mo_2C from negative to positive, while that of V_6C_5 remains negative, albeit higher.

The hydride formation enthalpies of all three metal carbides increase in the compressed state, with V_6C_5 hydride maintaining a (slightly) negative formation energy. Cr_7C_3 and Mo_2C hydride formation energies decrease to negative values in tense state. Notably the case for V_6C_5 is the opposite, although the formation energy remains negative despite its rise. The conclusion is that compressive strain will decrease both the stability and the hydrogen absorption ability of the metal carbides, while tensile strain will decrease the stability of metal carbides, but increase hydrogen absorption ability of the metal carbides in the alloy, with the exception of vanadium carbide.